Thermodynamic and kinetic control over the oxidation mechanism of the natural vanadyl porphyrin series (DPEP)VO in methylene chloride: electrogeneration of an unusual dicationic species $[(DPEP)VO]_2^{2+}$

Anass Doukkali,*[a] Ahmed Saoiabi,[b] Mohamed Ferhat,[b] Yves Mugnier,[c] Alain Vallat[c] and Roger Guilard[d]

Received (in Montpellier, France) 13th September 2005, Accepted 20th February 2006
First published as an Advance Article on the web 22nd May 2006
DOI: 10.1039/b512360g

The electrochemical behavior of the natural (DPEP)VO series (where DPEP is the dianion deoxophylloerythroetioporphyrinate) is studied in methylene chloride. The investigated compounds, which were extracted from oil shales of Tarfaya (Morocco), exhibit a typical electrochemical behavior as compared to that of related synthetic vanadyl porphyrins. The electro-oxidation of (DPEP)VO is characterized by a splitting of the peaks when carried out at a glassy carbon electrode. This can be explained by two possible paths (CE and EC mechanisms) which are characterized by a ''square diagram'' where the chemical step, C, corresponds to a dimerization (radical–radical or substrate–substrate reaction). The electrochemical or chemical ($AgBF_4$) oxidation gives a dimeric dicationic species $[(DPEP)VO]_2^{2+}$ which was characterised by EPR and UV-visible spectroscopy. Modelling of the current–voltage curves was carried out and all thermodynamic and kinetics parameters relative to the proposed square diagram were determined.

Introduction

The redox reaction in metalloporphyrin series mainly involves either the central metal ion or the conjugated π-ring system of the macrocycle. Some singly oxidized porphyrin π-cation radicals might be converted to singly oxidized or half-oxidized π–π dimers while others will not, depending in part on the overall planarity of the macrocycle, the solvent conditions and the nature of the particular porphyrin ring substituents.[1]

The one-electron oxidation reaction of metalloporphyrins have given rise to products which have been studied by paramagnetic resonance (EPR) and optical spectroscopy.[2] Some interesting situations arise when porphyrins are coordinated to transition metals such as vanadium, oxidation of which leads generally to a system containing an unpaired electron on the π ligand and one on the metal.[3]

Vanadium porphyrins have been characterized almost exclusively as V(IV) complexes. The electrochemistry of (P)VO derivatives and characterization of the oxidation or reduction products have been studied by many groups.[4] Each vanadyl complex generally undergoes two well defined reactions at the porphyrin π-ring system, leading in almost all cases to stable π-cation radicals and dications upon oxidation and stable π-anion radicals and dianions upon reduction. The typical example of vanadyl complexes is vanadyl tetraphenylporphyrin (TPP)VO. The electrooxidation reactions are reversible as evidenced by the peak-to-peak differences observed in the cyclic voltammograms. However, it was observed that the cation radical can dimerize at low temperature. In particular, the vanadyl octaethylporphyrin cation radical $[(OEP)VO]^+$ gives rise to a dimer ($S = 1$) at 80 K, in which the two π electrons are paired and the unpaired electrons are located in the vanadium orbitals.[5] A dimerization reaction was also considered for the proto- and mesoporphyrins for which the cyclic voltammograms present a splitting of the peak at the first oxidation step attributable to the presence of aggregates or dimers. The following mechanism was proposed to explain these data:[5]

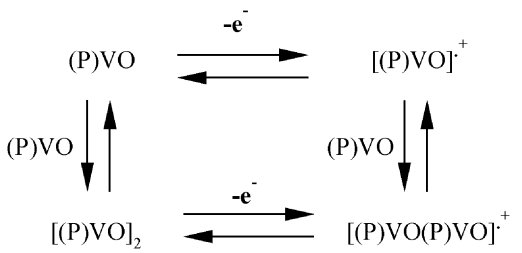

P = protoporphyrin or mesoporphyrin

the dimerisation can occur either before (substrate–substrate type reaction) or after (radical–substrate type reaction) the oxidation. The cationic dimer $[(proto)VO(proto)VO]^{\bullet+}$ and the corresponding analogous mesoporphyrin possess three unpaired electrons corresponding to a $S = 3/2$ state, one

[a] *Centre National de l'Energie des Sciences et des Techniques Nucléaires (CNESTEN), BP 1382, RP-Rabat, Maroc*
[b] *Laboratoire de Chimie Physique Générale, Faculté des Sciences, Université Mohamed-V-Agdal, av. Ibn Batouta, BP 1034, Rabat, Maroc*
[c] *Laboratoire de Synthèse et d'Electrosynthèse Organométallique (LSEO), UMR 5188, Faculté des Sciences Gabriel, Université de Bourgogne, 21000 Dijon, France*
[d] *Laboratoire d'Ingénierie Moléculaire pour la Séparation et les Applications des Gaz (LIMSAG), UMR 5633, Faculté des Sciences Gabriel, Université de Bourgogne, 21000 Dijon, France*

electron is localized in the porphyrin π molecular orbital and the others in each of the vanadium d_{xy} orbitals.[5]

Recent studies concerning corrole series report the electrogeneration of dimers in their singly and doubly oxidized forms.[6,7] For example, the first two oxidations of (OEC)M where M = Co, Ni or Cu[6] lead to $[(OEC)M]_2^+$ and $[(OEC)M]_2^{2+}$.

Many earlier works, carried out on a variety of porphyrin derivatives that differ in metal ion, axial ligation and/or porphyrin ligand, have showed differences in spin coupling between metal and porphyrin spins.[8–13] Both intra- and intermolecular spin-coupling can be significant. Vanadyl porphyrinates could be ideally simple systems that provide quantitative characterization of the combined effects of intra- and intermolecular spin-coupling.[14] Thus, the solution EPR spectra of $[VO(OH_2)(OEP^{\bullet})]SbCl_6$ ($SbCl_6^-$ is counterion), at high and low temperatures, show vanadium hyperfine splitting. The room-temperature spectrum (with eight lines) has been interpreted in terms of an intramolecular coupling process, while the low-temperature spectrum (fifteen lines with $g_\perp$ and $g_\parallel$ branches) result from a vanadium–vanadium triplet as a consequence of forming a strongly coupled cation radical dimer.[3,5,14]

In the present study, we report the electrochemistry of a natural DPEP vanadyl porphyrin series (see Chart 1, where DPEP is the dianion deoxophylloerythroetioporphyrinate) which was extracted by $CHCl_3$ from the Tarfaya (Morocco) oil shales. These porphyrins are present in the form of mixtures of homologous series.[15] Their electrochemical study seems to be complex, contrary to the synthetic models where the initial product is well known.[16–18] Nevertheless, the first measurements of cyclic voltammetry carried out on these complexes show an homogeneous electrochemical behavior, relating to only one entity. This can be explained by the fact that DPEP series is represented by only three principal homologous series ($C_{30}H_{30}N_4VO$, $C_{31}H_{32}N_4VO$, $C_{32}H_{34}N_4VO$) which differ solely by the number of methyl groups substituted on the porphyrin ring.[15]

The electrochemical study of the (DPEP)VO series was realized in a non-binding solvent, methylene chloride (CH_2Cl_2). Tetrabutylammonium hexafluorophosphate, $TBAPF_6$ (0.2 M) was used as supporting electrolyte, because this derivative can be easily purified and PF_6^- can be considered as non-binding or very weakly binding anion.

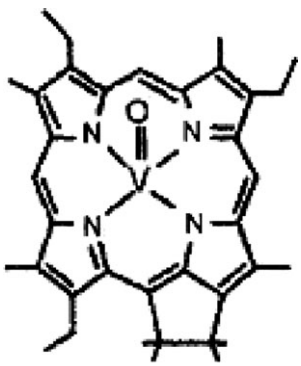

Vanadyl DPEP porphyrin

Chart 1

Experimental

Chemicals

The methylene chloride (CH_2Cl_2 *per analysis*) used in the electrochemical studies is purified by being passed over alumina, dehydrated beforehand under vacuum at 120 °C, then deoxygenated immediately before use. The tetrabutylammonium hexafluorophosphate used as supporting electrolyte was prepared by adding 75 ml of aqueous tetrabutylammonium hydroxide (40%) to 15 ml of aqueous hexafluorophosphoric acid (75%). The obtained solution was left under agitation for a few minutes; after filtration, the recovered supporting electrolyte was recrystallised three times from ethanol, then dried in an oven and finally vacuum deoxygenated before use.

Instrumentation

Voltammetric measurements were carried out using a Tacussel GSTP4&PJT24-1 unit connected to a Sefram TGM 101 plotting table. A conventional three-electrode cell, maintained under nitrogen current, was used and consisted of a glassy carbon electrode (3 mm in diameter) as a working electrode, a platinum wire as counter electrode and a saturated calomel reference electrode (SCE). The SCE was separated from the solution by a fritted glass bridge of low porosity that contained the solvent and the supporting electrolyte. Electrolysis were carried out using an Amel 552 potentiostat and an Amel 721 electronic integrator.

UV-visible spectra were recorded on a Varian Carry 5 spectrophotometer using 10^{-6} M solutions of materials. UV-visible spectroelectrochemical experiments were performed with a Tracor Northen 6500 multichannel analyser using a light-transparent platinum gauze as working electrode.

EPR spectra were recorded at room temperature in methylene chloride solution with a Bruker ESP 300 instrument operating in the X-band. The *g*-values were measured relative to dpph radical ($g = 2.0037 \pm 0.0003$).

Numerical simulation

The computations were performed using the commercially available program Digisim (Bioanalytical systems). The potential increase was set to 5 mV. The uncompensated resistance, here $R_u = 1000\ \Omega$, was determined with a PAR 373A potentiostat using the same experimental conditions as for the CV measurements. The double-layer capacitance value was estimated as $Cdl/A = 10^{-4}$ F cm^{-2} using a blank solution prior to voltammetric measurements. The experimental curves were corrected for residual current, also determined using voltammetric measurements of blank solutions.

Results and discussion

The rotating disk electrode voltammogram of (DPEP)VO series, presents three waves: two oxidation waves O'_1 and O'_2 and one reduction wave R_1 (Fig. 1, Table 1). As the intensity of these waves is nearly equal, the overall process can be rationalised according to the redox following reactions (1). The calculation of the slopes of the $\ln(I/I_l - I) = f(E)$ curves in the case of oxidations and $\ln(I_l - I/I) = f(E)$ curve in the

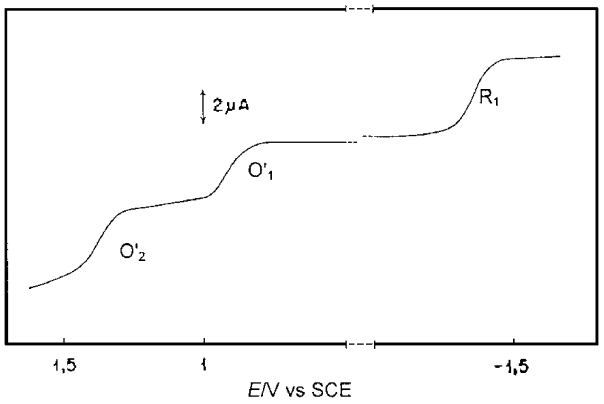

Fig. 1 Rotating disk electrode voltammogram of (DPEP)VO series in CH_2Cl_2; $v = 10$ mV s^{-1}.

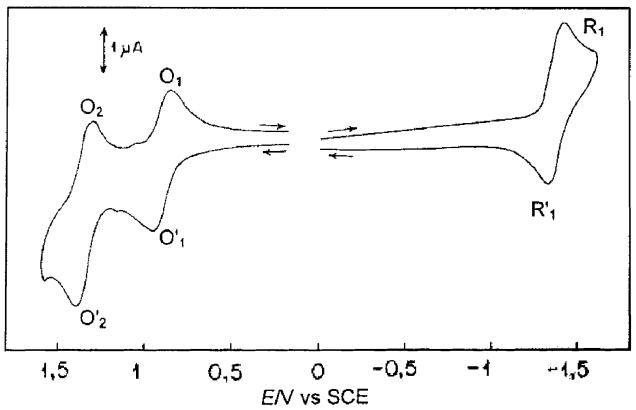

Fig. 2 Cyclic voltammogram of (DPEP)VO series in CH_2Cl_2, $v = 20$ mV s^{-1}.

case of reduction, gives 0.86 and 1.12, respectively, as a number of electrons exchanged for the two systems of oxidation and 0.99 for the system of reduction.

$$[(DPEP)VO]^{2+} \xrightarrow{O'_2} [(DPEP)VO]^{+} \xrightarrow{O'_1} (DPEP)VO \xrightarrow{R_1} [(DPEP)VO]^{-} \quad (1)$$

In the anodic field, the cyclic voltammogram of (DPEP)VO series shows O_1/O'_1 and O_2/O'_2 systems at $E_{1/2} = 0.90$ and 1.35 V (Fig. 2), respectively. The difference in potential ΔE_p between the two oxidation waves is about 0.45 V, which has often been used to predict that the two oxidations are centered on the conjugated porphyrin ring.[19] The peak current I_P of the first oxidation step does not increase linearly with the square root of scan rate, which indicates this oxidation reaction is not diffusion-controlled.

For the second oxidation step, the value $\Delta E_p = |E_P - E_{P/2}| = (70 \pm 5)$ mV is not very different from the theoretical value $(56.5/n)$ mV. The half-wave potential is independent of scan rate and the peak current increases linearly with the square root of scan rate which indicates a diffusion-controlled one-electron reversible oxidation process.

In the cathodic field, the cyclic voltammogram of (DPEP)-VO series shows a R_1/R'_1 system at $E_{1/2} = -1.37$ V (Fig. 2). The value $\Delta E_p = |E_P - E_{P/2}| = (70 \pm 5)$ mV is close to the theoretical value which is about $(56.5/n)$ mV. In the other hand, the half-wave potential is independent of scan rate and the peak current increases linearly with the square root of scan rate, indicating thus, a diffusion-controlled one-electron reversible process of reduction. The full investigation of the reduction process in DMF or CH_2CL_2 will be published later.[20] The above results can be rationalised according to the following redox reactions (2).

$$[(DPEP)VO]^{2+} \overset{O'_2/O_2}{\rightleftharpoons} [(DPEP)VO]^{+} \overset{O'_1/O_1}{\rightleftharpoons} (DPEP)VO \overset{R_1/R'_1}{\rightleftharpoons} [(DPEP)VO]^{-} \quad (2)$$

Table 1 Half-wave potentials and intensities of the oxidoreduction waves of (DPEP)VO series

	Ox_1 (O'_1)	Ox_2 (O'_2)	Red_1 (R_1)
$E_{1/2}$/V (*vs.* SCE)	0.92	1.38	−1.36
I_l/μA	3.6	3.2	4.9

First oxidation step

For the first oxidation step, the voltammogram morphology depends on scan rate and temperature; we have observed a splitting of the redox peaks of the first system with the appearance of two new systems (O_1/O'_1 and O_1^*/O'_1^*) (Fig. 3(a)). Thus, when the scan rate increases, the second oxidation peak O'_1^* becomes more intense compared to O'_1. At reverse scan, the peak of reduction O_1^* increases with the scan rate as well, but remains much less intense than O_1 (Fig. 3(a)). At low temperature, the intensities of the peaks O'_1^* and O_1^* increase relatively compared to the peaks O'_1 and O_1 (Fig. 3(b)).

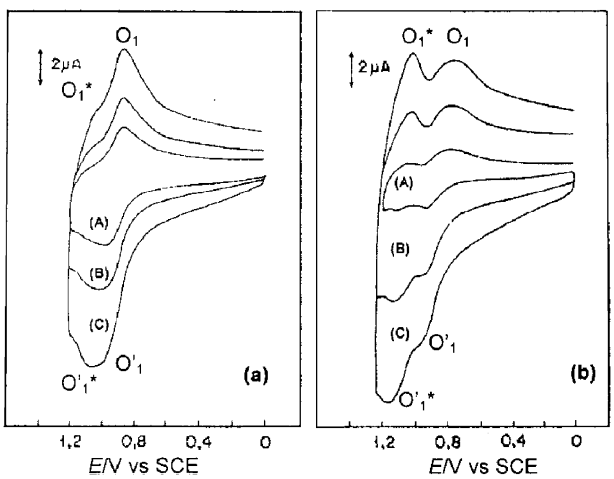

Fig. 3 Cyclic voltammograms of DPEP(VO) series ($C = 5 \times 10^{-4}$ mol L^{-1}) in CH_2Cl_2: (a) at room temperature; scan rate: (A) $v = 50$ mV s^{-1}; (B) $v = 150$ mV s^{-1}; (C) $v = 250$ mV s^{-1}. (b) $T = -78$ °C; scan rate: (A) $v = 50$ mV s^{-1}; (B) $v = 250$ mV s^{-1}; (C) $v = 550$ mV s^{-1}.

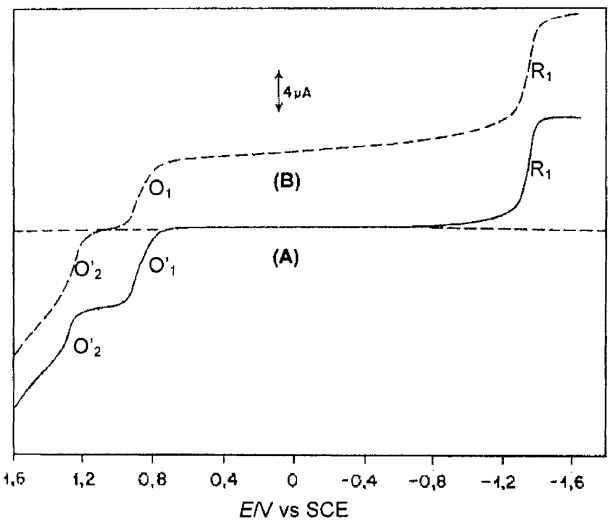

Fig. 4 Rotating disk electrode voltammograms of (DPEP)VO series in CH_2Cl_2 with v = 20 mV s^{-1}: (A) before electrolysis, (B) after electrolysis at 1 V.

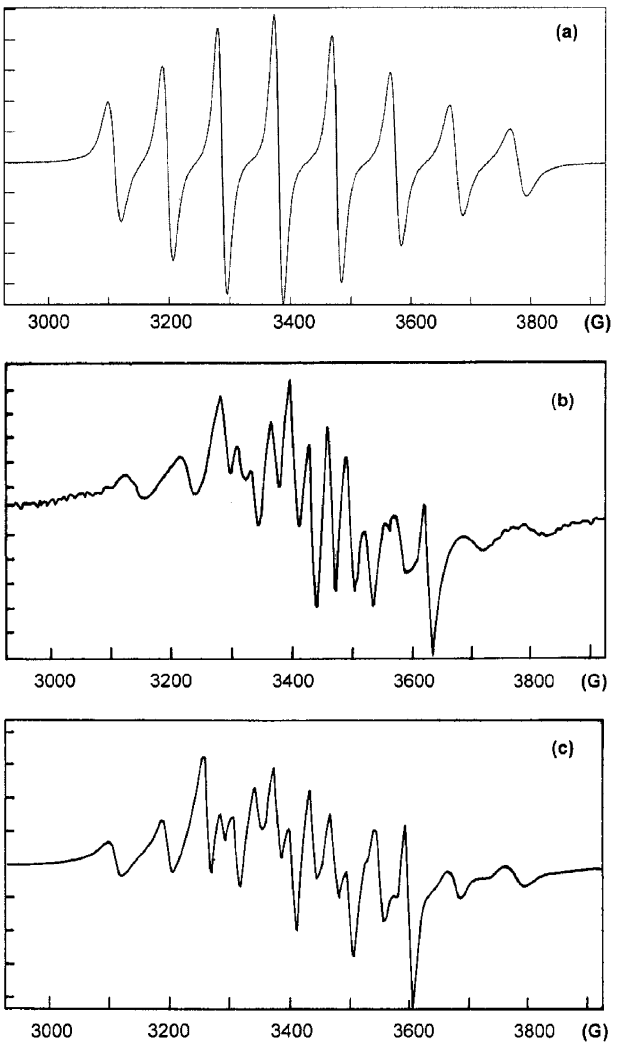

Fig. 5 (a) EPR spectrum at room temperature of (DPEP)VO series in CH_2Cl_2; (b) EPR spectrum at room temperature, after electrolysis at 1 V, of (DPEP)VO series in CH_2Cl_2; (c) EPR spectrum at room temperature in CH_2Cl_2 of the product of the chemical oxidation of (DPEP)VO series by $AgBF_4$.

These results suggest that the mechanism is not limited to a simple one-electron transfer process because chemical reactions probably occur during the oxidation process.

Electrolysis at 1 V indicates that the process corresponds to one-electron-transfer (n_{exp} = 0.85 F mol^{-1}) thus confirming the results detailed above. The rotating disk electrode voltammetry of the electro-generated compound presents the oxidation wave O'_2 and the reduction waves O_1 and R_1 (Fig. 4). By cyclic voltammetry, only one system (O_1/O'_1) is observed. The electrogenerated product is relatively unstable and leads gradually to the regeneration of the initial compound (the wave of reduction O_1 decreases and the oxidation wave O'_1 reappears, then increases).

This instability of the oxidation product, even at low temperature, made difficult its characterisation in a precise way. Nevertheless, EPR spectrum of the oxidation product presents two superimposed signals, which is characteristic of a mixture of the initial compound and the oxidation product (Fig. 5(b)). A similar spectrum is also obtained by carrying out chemical oxidation of (DPEP)VO series using $AgBF_4$ (Fig. 5(c)). This spectra with a significant number of lines and a value of the hyperfine coupling constant A_{iso} = 32.7 G can be explained only by assuming the interaction of two vanadium nuclei with unpaired electrons. This species can be viewed as a dimer $[(DPEP)VO]_2^{2+}$ formed by two radical cations of (DPEP)VO. A similar dimerization has been reported for the radical cation of (OEP)VO.[5]

The UV-visible spectra recorded during a potential scan from 0.7 to 1.1 V (Fig. 6), does not show any broad band towards longer wavelengths ($\lambda \leq$ 750 nm). However, we have noticed a significant decrease of the Soret band and the appearance of a shoulder towards the blue which becomes a whole band appearing at 393 nm. This band decreases further while another band appears in the UV region (358 nm). The Q bands at 531 and 572 nm also disappear. This spectral morphology can be compared to that of (proto)VO where oxidation leads to an unstable dimeric compound.[5] These characteristics are not in agreement with the simple formation of a cation radical but correspond to the generation of dicationic dimer, which is in concordance with the results of EPR spectroscopy.

Furthermore, the cyclic voltammetry data suggest several oxidation processes of (DPEP)VO series for which chemical reactions are coupled with electron transfers (CE and/or EC mechanisms). These chemical steps correspond to a radical–radical or substrate–substrate type dimerization. The assumption of a radical–substrate type dimerization is not possible because the dimer $[(DPEP)VO]_2^+$ should be obtained according to a 0.5 F process.

The global mechanism can be represented by the following "square diagram" (Scheme 1) which was suggested at the first time by Jacq in organometallic chemistry.[21]

At low scan rate, (DPEP)VO is oxidised according to a CE mechanism (O'_1 peak) (path a–b–c) for which the chemical step yields $[(DPEP)VO]_2$ by (DPEP)VO dimerization. Even

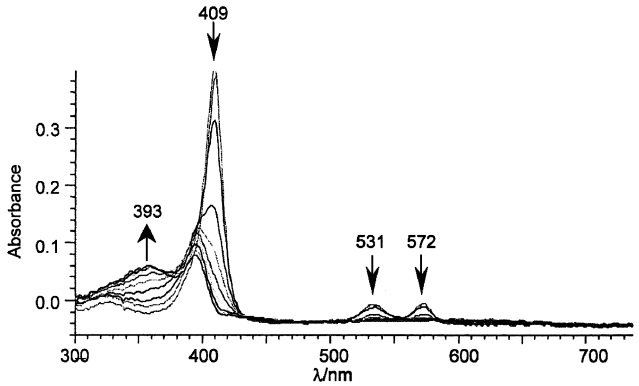

Fig. 6 Electronic absorption spectra during potential scan from 0.7 to 1.1 V of 4×10^{-4} mol L^{-1} (DPEP)VO series in CH_2Cl_2; v = 100 mV s^{-1}.

though dimer formation constant K_2 = $[((DPEP)VO)_2]/[(DPEP)VO]^2$ should be very weak (*cf.* simulation data), this reaction is made possible by the following electrochemical reaction. The O_1 peak corresponds to the reduction of $[(DPEP)VO]_2^{2+}$ to $[(DPEP)VO]_2$ (path c–b) (see below). The fact that the dimer is oxidised more easily than the corresponding monomer and the appearance of only one system (O_1/O'_1) after electrolysis are in agreement with the proposed process.

At low temperature and/or high scan rate, this dimerization cannot occur due to a decrease of the kinetics. Consequently, (DPEP)VO is oxidized to give $[(DPEP)VO]^+$ (O'_1* peak) which leads to the derivative $[(DPEP)VO]_2^{2+}$ by dimerisation reaction (path a–d–c).

These assumptions (substrate–substrate and/or radical–radical type dimerization) were confirmed by the electrochemical study of (DPEP)VO series at various concentrations. At high concentrations ($C = 8.3 \times 10^{-3}$ mol L^{-1}; Fig. 7(a)), only one system (O_1/O'_1) is observed; the difference in potential $\Delta E = E_pO'_1 - E_pO_1$ = 170 mV is much higher than the theoretical value corresponding to a reversible two-electron process (ΔE = 30 mV). Such a difference (ΔE = 0.2 V) was already mentioned in the case of oxidation of the (OEP)VO complex,[22] which is a synthetic porphyrin used generally as a model of natural porphyrins. Under these conditions, the difference in potential observed between O'_1 and O_1 indicates that the followed forward and backward pathways are then different: CE process for oxidation (path a–b–c) at O'_1 and purely electrochemical process for the reduction at O_1 (path c–b). No splitting is observed with the scan rate (from 0.025 to

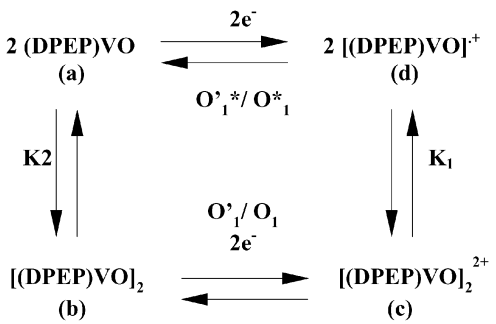

Scheme 1

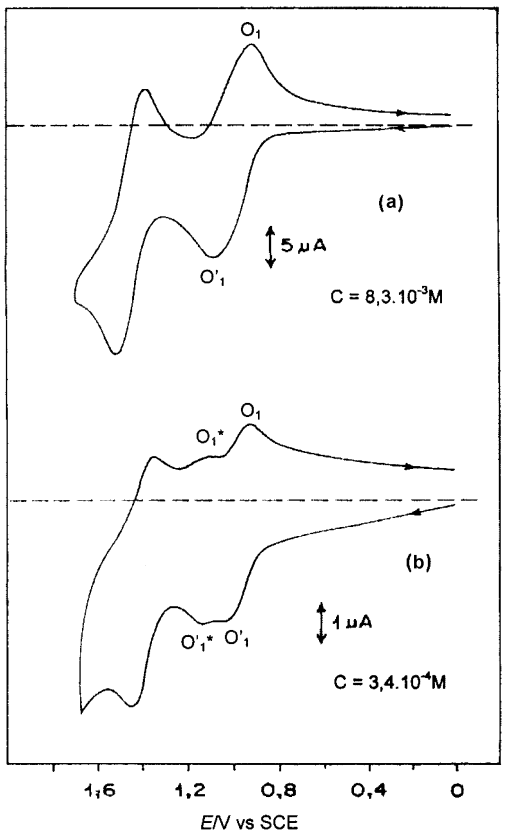

Fig. 7 Cyclic voltammograms of (DPEP)VO series in CH_2Cl_2 at various concentrations.

1 V s^{-1}) and with the temperature (from 20 to −46 °C). By dilution (Fig. 7(b)), a second system (O_1*/O'_1*) appears, the intensities of the peaks increase gradually by dilution compared to the peaks of the first system (O_1/O'_1).

If the electrochemical data indicate clearly the monomer–dimer equilibrium, it was not possible, however, to demonstrate precisely the phenomenon of dimerization by electronic absorption. However, at high concentration ($C = 10^{-2}$ mol L^{-1}), a decrease in the molar extinction coefficient and a broadening of the Soret band were noticed. This spectral morphology was already raised for some porphyrin complexes, due to the formation of aggregates.[23,24]

The attribution of the second system (O_1*/O'_1*) corresponding to the following redox reaction (3) was confirmed by the study of the product obtained during the oxidation of (DPEP)VO series by CF_3CO_2H (trifluoroacetic acid).

$$(DPEP)VO \overset{-e^-}{\rightleftharpoons} [(DPEP)VO]^+ \qquad (3)$$

The oxidation of (DPEP)VO by CF_3CO_2H yields the $[(DPEP)VO]^+$ radical characterized by EPR spectroscopy. The obtained spectrum at room temperature in CH_2Cl_2, gives isotropic parameters (g_{iso} = 1.998, A_{iso} = 46 G) (Fig. 8). This spectrum is similar to that of $[(OEP)VO]^+$ with eight lines with a hyperfine coupling constant indicating an interaction between the two unpaired electrons.[25] According to cyclic voltammetry, $[(DPEP)VO]^+$ (prepared chemically), presents only the O_1*/O'_1* system.

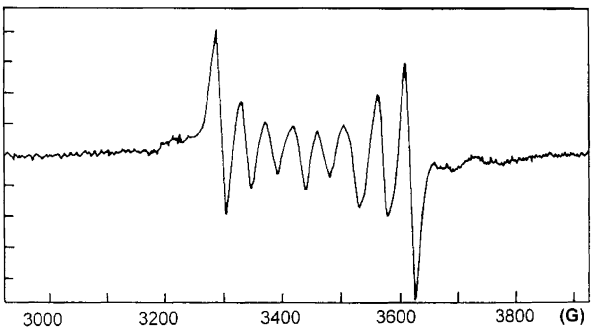

Fig. 8 EPR spectrum at room temperature of the $[(DPEP)VO]^+$ radical in methylene chloride obtained from chemical oxidation of (DPEP)VO by CF_3CO_2H (trifluoroacetic acid).

During this study, we have noticed that chemical oxidation of (DPEP)VO by CF_3CO_2H leads always to $[(DPEP)VO]^+$ even at high concentration, whereas by electrochemical oxidation the dimer $[(DPEP)VO]_2^{2+}$ is obtained.

It is difficult to specify exactly the reasons for which different products are obtained with the used method. The nature of the counterion CF_3COO^- used in the chemical synthesis can be one of he invoked parameters. The interaction between $[(DPEP)VO]^+$ and CF_3COO^- can be relatively strong and thus limits the evolution of $[(DPEP)VO]^+$ to $[(DPEP)VO]_2^{2+}$. On the other hand, by electrochemical route, the presence of PF_6^- (inert anion) can favour this dimerization by recovery of the coupling orbitals of the π-porphyrin rings. Moreover, the oxidation of (DPEP)VO by $AgBF_4$ seems to favour the dimer $[(DPEP)VO]_2^{2+}$ formation, which is supported by the weak capacity of coordination of the BF_4^- anion.

The simulation of the current–voltage curves allows us to determine all thermodynamic and kinetic parameters relative to the proposed "square diagram".

Second oxidation step

The two-electron oxidized complex was generated by electrolysis of (DPEP)VO at 1.4 V (1.82 F mol^{-1} of (DPEP)VO). The analysis by EPR spectroscopy shows that the spectrum of the product obtained at the second oxidation of (DPEP)VO is similar to that of the initial complex. This result indicates that extraction of the second electron on the porphyrin macrocycle led to the $[(DPEP)VO]^{2+}$ dication (eqn (4)).

$$(DPEP)VO \xrightarrow{-2e^-} [(DPEP)VO]^{2+} \qquad (4)$$

It is interesting to note that the addition of acetonitrile to the porphyrin solution does not modify the two systems (O_1/O'_1 and O_1^*/O'_1^*), but induces a cathodic shift (ΔE = 200 mV) of the second system (O_2/O'_2). This shift is attributed to the coordination of acetonitrile on the porphyrin complex after removal of the second electron which confirms the formation of $[(DPEP)VO]^{2+}$ dication at the second step (eqn (5)).

$$(DPEP)VO - 2e^- \rightarrow [(DPEP)VO]^{2+}$$
$$[(DPEP)VO]^{2+} + ACN \rightleftharpoons [(DPEP)VO(ACN)]^{2+} \qquad (5)$$

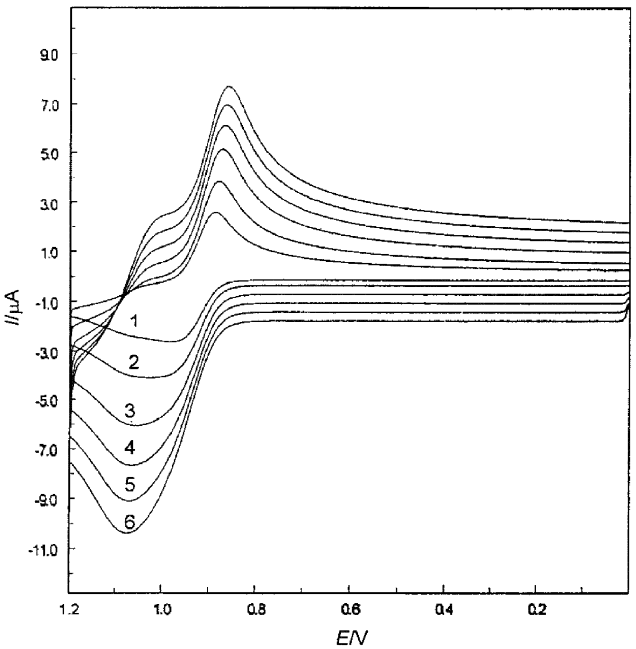

Fig. 9 Simulated cyclic voltammograms of 5×10^{-4} mol L^{-1} of (DPEP)VO series in CH_2Cl_2; influence of scan rate: v = 20 (1), 50 (2), 100 (3), 150 (4), 200 (5), 250 mV s^{-1} (6).

Simulation

To explain the electrochemical oxidation of the (DPEP)VO series, the following mechanism represented in the form of a "square diagram",[26–28] is suggested (Scheme 2). The chemical reactions of the dimerisation reaction are indicated in the vertical direction.

With $E^\circ_1 > E^\circ_2$ and A = (DPEP)VO, $K_1 = k_{f1}/k_{b1} = [A–A^{2+}]/[A^+]^2$, $K_2 = k_{f2}/k_{b2} = [A–A]/[A]^2$.

The constants K_1 and K_2 are linked to the difference in potential $\Delta E = E^\circ_2 - E^\circ_1$ by the relation: $K_2/K_1 = \exp[2F(E^\circ_2 - E^\circ_1)/RT]$.

The condition $E^\circ_1 > E^\circ_2$ invokes that $K_1 > K_2$. When K_2 is not so large, the $2A \rightleftharpoons A–A$ equilibrium can be moved in favour of A–A under influence of its oxidation, which confirms the existence of the two O'_1 and O'_1* oxidation peaks. If the difference in potential is significant, K_1 is then large and the equilibrium $2A^+ \rightleftharpoons A–A^{2+}$ is moved in favour of the formation of $A–A^{2+}$ as a result the O_1 peak is then dominating.

The simulated curves at various scan rates are given on Fig. 9 (the experimental curves are those of Fig. 3(a)). On the basis

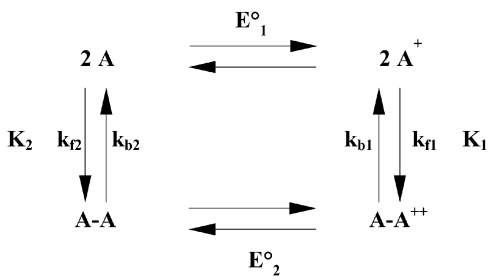

Scheme 2

of these data, a good correlation is obtained applying values $E^{\circ}_1 = 1.04$ V and $E^{\circ}_2 = 0.88$ V.

Electron-transfer rate constants k_{S1} and k_{S2} were fixed at 2×10^{-2} cm s^{-1} (values obtained before in the case of nickel porphyrin complexes under the same operating conditions).[29] The same behavior is assumed for the proposed diffusion coefficient, $D = 6 \times 10^{-6}$ cm^2 s^{-1}.[30]

The equilibrium constant K_2 is not very large; a good approximation is obtained for $K_2 = 40$ mol^{-1} L. The relation existing between K_1, K_2, E°_1 and E°_2 led to a high value of K_1 ($K_1 = 1.024 \times 10^7$ mol^{-1} L), which confirms the stability of A–A^{2+}.

The rate constants k_{f2} and k_{b2} are not thus very different and must be relatively higher to explain the maintenance of the first system (O_1/O'_1) at high scan rate. On the other hand, k_{b1} must be low, because the O_1* peak is visible only at high scan rate. A good approximation is obtained for $k_{f2} = 10^8$ mol^{-1} L s^{-1}, $k_{b2} = 2.5 \times 10^6$ s^{-1} and $k_{f1} = 10^3$ mol^{-1} L s^{-1}, $k_{b1} = 9.7 \times 10^{-5}$ s^{-1}.

Conclusion

The study of the electrochemical behaviour of the natural porphyrin (DPEP)VO in methylene chloride has shown some particular and original aspects compared to those of synthetic complexes of vanadyl porphyrins mentioned in the literature.

On the basis of electrochemical, spectroelectro-chemical and EPR data, we could specify a radical–radical type dimerization reaction yielding an unusual dicationic species [(DPEP)-VO]$_2^{2+}$. The splitting of the peaks when carried out at a glassy carbon electrode was explained by two possible paths (CE and EC mechanisms) which are explained by a ''square diagram''. This scheme has also been confirmed by the simulation of the current–voltage curves which allows the determination of all thermodynamic and kinetic parameters relative to the proposed ''square diagram''.

Acknowledgements

A. D. is greatly indebted to Dr J. M. Barbe and Dr D. Lucas for their steady interest during this research and for many helpful discussions.

References

1 K. M. Kadish, E. Van Caemelbecke and G. Royal, in *The Porphyrin Handbook*, ed. K. M. Kadish, K. M. Smith and R. Guilard, Academic Press, New York, 2000, vol. 8, ch. 55, p. 6.
2 R. H. Felton, in *The Porphyrins*, ed. D. Dolphin, Academic Press, New York, 1978, vol. 5, p. 53.
3 G. R. Luckhurst, M. Setaka and J. Subramanian, *Mol. Phys.*, 1976, **32**, 1299.
4 K. M. Kadish, E. Van Caemelbecke and G. Royal, in *The Porphyrin Handbook*, ed. K. M. Kadish, K. M. Smith and R. Guilard, Academic Press, New York, 2000, vol. 8, ch. 55, p. 27.
5 A. Lemtur, B. K. Chakravorty, K. D. Tripti and J. Subramanian, *J. Phys. Chem.*, 1984, **88**, 5603.
6 K. M. Kadish, V. A. Adamian, E. Van Caemelbecke, E. Gueletii, S. Will, C. Erben and E. Vogel, *J. Am. Chem. Soc.*, 1998, **120**, 11986.
7 (*a*) R. Guilard, C. P. Gros, F. Boltze, F. Jerome, Z. Ou, J. Shao, J. Fischer, R. Weiss and K. M. Kadish, *Inorg. Chem.*, 2001, **40**, 4845; (*b*) K. M. Kadish, J. Shao, Z. Ou, C. P. Gros, F. Boltze, J. M. Barbe and R. Guilard, *Inorg. Chem.*, 2003, **42**, 4062.
8 P. Gans, G. Buisson, E. Duée, J. C. Marchon, B. S. Erler, W. F. Scholz and C. A. Reed, *J. Am. Chem. Soc.*, 1986, **108**, 1223.
9 B. S. Erler, W. F. Scholz, Y. J. Lee, W. R. Scheidt and C. A. Reed, *J. Am. Chem. Soc.*, 1987, **109**, 2644.
10 H. Song, N. P. Rath, C. A. Reed and W. R. Scheidt, *Inorg. Chem.*, 1989, **28**, 1839.
11 H. Song, C. A. Reed and W. R. Scheidt, *J. Am. Chem. Soc.*, 1989, **111**, 6867.
12 (*a*) H. Song, C. A. Reed and W. R. Scheidt, *J. Am. Chem. Soc.*, 1989, **111**, 6865; (*b*) H. Song, R. D. Orosz, C. A. Reed and W. R. Scheidt, *Inorg. Chem.*, 1990, **29**, 4274.
13 W. R. Scheidt, H. Song, K. J. Haller, M. K. Safo, R. D. Orosz, C. A. Reed, P. G. Debrunner and C. E. Schultz, *Inorg. Chem.*, 1992, **31**, 939.
14 C. E. Schultz, H. Song, Y. J. Lee, J. U. Mondal, K. Mohanrao, C. A. Reed, F. A. Walker and W. R. Scheidt, *J. Am. Chem. Soc.*, 1994, **116**, 7196.
15 A. Doukkali, A. Saoiabi, A. Zrineh, M. Hamad, M. Ferhat, J. M. Barbe and R. Guilard, *Fuel*, 2002, **81**, 467.
16 K. M. Kadish, C. Araullo, B. G. Maiya, D. Sazou, J. M. Barbe and R. Guilard, *Inorg. Chem.*, 1989, **28**, 2528.
17 K. M. Kadish, D. Sazou, C. Araullo, Y. M. Liu, A. Saoiabi, M. Ferhat and R. Guilard, *Inorg. Chem.*, 1988, **27**, 2313.
18 K. M. Kadish, D. Sazou, Y. M. Liu, A. Saoiabi, M. Ferhat and R. Guilard, *Inorg. Chem.*, 1988, **27**, 686.
19 K. M. Kadish, *Prog. Inorg. Chem.*, 1987, **34**, 435.
20 A. Doukkali, A. Saoiabi, M. Ferhat, Y. Mugnier, A. Vallat and R. Guilard, unpublished work.
21 J. Jacq, *J. Electroanal. Chem.*, 1971, **29**, 149.
22 Y. O. Su, R. S. Czernuszervicz, L. A. Miller and T. G. Spiro, *J. Am. Chem. Soc.*, 1988, **110**, 4150.
23 (*a*) W. I. White, in *The Porphyrins*, ed. D. Dolphin, Academic Press, New York, 1978, vol. 5, ch. 5; (*b*) K. Kano, T. Najima, M. Takei and S. Hasimoto, *Bull. Chem. Soc. Jpn.*, 1987, **60**, 1281; (*c*) A. Corsini and O. Hermann, *Talanta*, 1986, **33**, 335.
24 N. Senglet, Thèse de l'Université de Bourgogne, Dijon, 1988.
25 J. Subramanian, in *Porphyrins and Metalloporphyrins*, ed. K. M. Smith, Elsevier, Amsterdam, 1975, p. 584.
26 (*a*) E. Laviron, *J. Electroanal. Chem.*, 1983, **1**, 146; (*b*) E. Laviron, *J. Electroanal. Chem.*, 1983, **15**, 146; (*c*) E. Laviron and R. Meunier, *J. Electroanal. Chem.*, 1992, **1**, 324; (*d*) E. Laviron and R. Meunier, *J. Electroanal. Chem.*, 1992, **33**, 328.
27 E. Laviron and L. Roullier, *J. Electroanal. Chem.*, 1985, **1**, 186.
28 A. Vallat, L. Roullier and C. Bourdon, *J. Electroanal. Chem.*, 2003, **75**, 542, and references therein.
29 D. Chang, T. Malinski, A. Ulman and K. M. Kadish, *Inorg. Chem.*, 1984, **23**, 817.
30 K. M. Kadish and C. H. Su, *J. Am. Chem. Soc.*, 1983, **105**, 177.